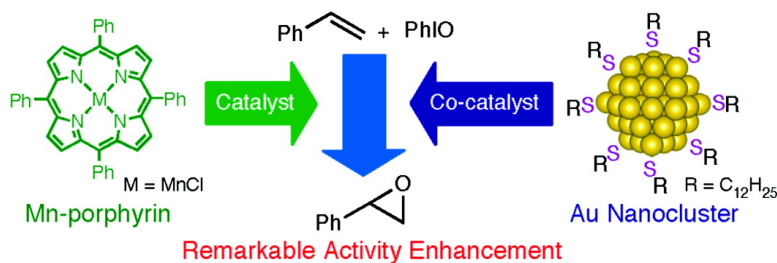


## Remarkable Co-catalyst Effect of Gold Nanoclusters on Olefin Oxidation Catalyzed by a Manganese–Porphyrin Complex

Yoshitaka Murakami, and Katsuaki Konishi

*J. Am. Chem. Soc.*, **2007**, 129 (46), 14401-14407 • DOI: 10.1021/ja075051b • Publication Date (Web): 30 October 2007

Downloaded from <http://pubs.acs.org> on February 13, 2009



### More About This Article

Additional resources and features associated with this article are available within the HTML version:

- Supporting Information
- Links to the 4 articles that cite this article, as of the time of this article download
- Access to high resolution figures
- Links to articles and content related to this article
- Copyright permission to reproduce figures and/or text from this article

[View the Full Text HTML](#)

## Remarkable Co-catalyst Effect of Gold Nanoclusters on Olefin Oxidation Catalyzed by a Manganese–Porphyrin Complex

Yoshitaka Murakami and Katsuaki Konishi\*

Contribution from the Creative Research Initiative 'Sosei' and Graduate School of Environmental Science, Hokkaido University, North 21 West 10, Sapporo 001-0021, Japan

Received July 9, 2007; E-mail: konishi@ees.hokudai.ac.jp

**Abstract:** The effect of dodecanethiolate-protected metallic nanoclusters of gold (Au:SC12, **1**), silver (Ag:SC12), palladium (Pd:SC12), and platinum (Pt:SC12) on the catalytic activity of Mn(TPP)Cl (TPP = tetraphenylporphyrinato) was investigated in styrene oxidation with iodobenzene. Among the four metal clusters, only Au:SC12 led to appreciable acceleration of the catalytic reaction. The major role of the Au cluster was to regenerate the active catalytic path involving Mn(III) and Mn(V) from the deactivated Mn(IV) species. The binary **1**/Mn(TPP)Cl catalyst system showed an absorption spectrum characteristic of Mn(III)–porphyrin after reaction, whereas a catalytically ineffective Mn(IV) species was observed as the sole porphyrin species in the absence of the Au cluster or in the presence of Pd, Ag, and Pt clusters. Accordingly, the slow oxidation reaction with Mn(TPP)Cl was accelerated by the addition of Au:SC12, and complete conversion of Mn(IV) into Mn(III) was observed in the absorption spectrum. <sup>1</sup>H NMR inspection of the reaction of Au:SC12 and iodobenzene revealed that the surface dodecyl groups were partially oxidized into dodecanal and eliminated from the cluster surface, thereby producing unprotected gold sites on the surface. A reactivation mechanism involving the reaction of the Mn–porphyrin and the oxidant activated on the gold surface is proposed.

### Introduction

Since the pioneering work by Haruta, the prominent catalytic activity of gold nanoclusters has attracted special attention, not only in its fundamental aspects but also in relation to practical chemical syntheses.<sup>1</sup> Extensive studies have been continuing up to the present, especially on the aerobic oxidation of CO and alcohols in gas and liquid phases, revealing their distinctive capability to activate oxidants under mild conditions.<sup>2,3</sup> Such a unique feature may also arise in other oxidation catalytic systems. For example, the activity of a certain catalyst would be enhanced when gold clusters assist the oxidative formation of a reactive intermediate (e.g., high-valent species). However, such promoting effects of gold clusters have not been reported to date.

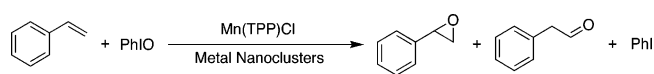
We herein studied Mn–porphyrin-catalyzed olefin oxidation as a model reaction and investigated the effects of metallic clusters on the reaction rate. Olefin oxidation catalyzed by manganese(III) complexes of porphyrin and related macrocycles

has been studied in relation to the mechanism of cytochrome P450 enzymes.<sup>4,5</sup> However, the catalytic turnovers are generally low due to the catalyst deactivation during the catalytic cycle: the oxoMn(V) intermediate, which is considered to be responsible for high activity,<sup>6</sup> is easily transformed into a less active Mn(IV) species,<sup>7</sup> resulting in low turnover numbers (TONs). It has also been suggested that the less active Mn(IV) species is labile and reverts to the reactive forms by the action of appropriate additives that induce redox perturbation (e.g., reduction, disproportionation).<sup>8</sup> Therefore, it is expected that gold clusters having high catalytic activity for oxidation may mediate these redox processes to improve the catalytic activity.

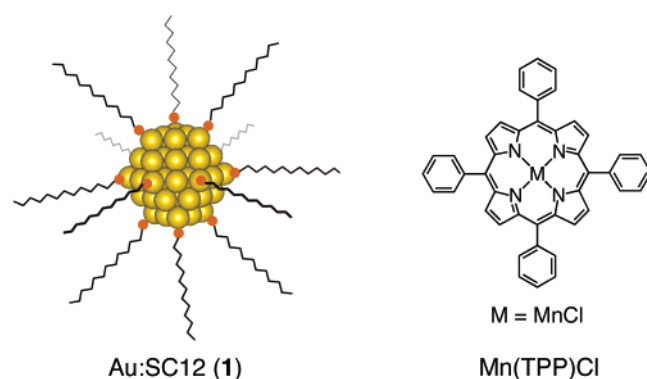
- (1) (a) Haruta, M.; Kobayashi, T.; Sano, H.; Yamada, N. *Chem. Lett.* **1987**, 405. (b) Haruta, M. *Nature* **2005**, *437*, 1098.
- (2) (a) Astruc, D.; Lu, F.; Aranzas, J. R. *Angew. Chem., Int. Ed.* **2005**, *44*, 7852. (b) Hughes, M. D.; Xu, Y.-J.; Jenkins, P.; McMorn, P.; Landon, P.; Enache, D. I.; Carley, A. F.; Attard, G. A.; Hutchings, G. J.; King, F.; Stitt, E. H.; Johnston, P.; Griffin, K.; Kiely, C. J. *Nature* **2005**, *437*, 1132. (c) Chowdhury, B.; Bravo-Suarez, J. J.; Date, M.; Tsubota, S.; Haruta, M. *Angew. Chem., Int. Ed.* **2006**, *45*, 412. (d) Bokhoven, J. A. van.; Louis, C.; Miller, J. T.; Tromp, M.; Safonova, O. V.; Glatzel, P. *Angew. Chem., Int. Ed.* **2006**, *45*, 4651.
- (3) (a) Comotti, M.; Pina, C. D.; Matarrese, R.; Rossi, M. *Angew. Chem., Int. Ed.* **2004**, *43*, 5812. (b) Tsunoyama, H.; Sakurai, H.; Ichikuni, N.; Negishi, Y.; Tsukuda, T. *Langmuir* **2004**, *20*, 11293. (c) Tsunoyama, H.; Sakurai, H.; Negishi, Y.; Tsukuda, T. *J. Am. Chem. Soc.* **2005**, *127*, 9374.

- (4) (a) Meunier, B. *Chem. Rev.* **1992**, *92*, 1411. (b) Dolphin, D.; Traylor, T. G.; Xie, L. Y. *Acc. Chem. Res.* **1997**, *30*, 251. (c) Katsuki, T. *Coord. Chem. Rev.* **1995**, *140*, 189.
- (5) (a) Hill, C. L.; Schardt, B. C. *J. Am. Chem. Soc.* **1980**, *102*, 6374. (b) Groves, J. T.; Kruper, W. J.; Haushalter, R. C. *J. Am. Chem. Soc.* **1980**, *102*, 6375. (c) Guilmet, E.; Meunier, B. *Tetrahedron Lett.* **1980**, *21*, 4449. (d) Battioni, P.; Renaud, J. P.; Bartolo, J. F.; Reina-Artiles, M.; Fort, M.; Mansuy, D. *J. Am. Chem. Soc.* **1988**, *110*, 6462. (e) Lee, R. W.; Nakagaki, P. C.; Bruce, T. C. *J. Am. Chem. Soc.* **1989**, *111*, 1368. (f) Groves, J. T.; Lee, J.; Marla, S. S. *J. Am. Chem. Soc.* **1997**, *119*, 6269. (g) Collman, J. P.; Zeng, L.; Decreau, R. A. *Chem. Comm.* **2003**, 2974.
- (6) The true active species is not yet clear, see: (a) Gross, Z.; Golublov, G.; Simkhovich, L. *Angew. Chem., Int. Ed.* **2000**, *39*, 4045. (b) Wang, S. H.; Mandimutsira, B. S.; Todd, R.; Ramdhanie, B.; Fox, J. P.; Goldberg, D. P. *J. Am. Chem. Soc.* **2004**, *126*, 18. (c) Song, W. J.; Seo, M. S.; George, S. D.; Ohta, T.; Song, R.; Kang, M.; Toshi, T.; Kitagawa, T.; Solomon, E. I.; Nam, W. *J. Am. Chem. Soc.* **2007**, *129*, 1268.
- (7) (a) Schardt, B. C.; Hollander, F. J.; Hill, C. L. *J. Am. Chem. Soc.* **1982**, *104*, 3964. (b) Groves, J. T.; Stern, M. K. *J. Am. Chem. Soc.* **1988**, *110*, 8638. (c) Park, S.-E.; Song, W. J.; Ryu, Y. O.; Lim, M. H.; Song, R.; Kim, K. M.; Nam, W. *J. Inorg. Biochem.* **2005**, *99*, 424.
- (8) (a) Merlau, M. L.; Cho, S.; Sun, S.; Nguyen, S. T.; Hupp, J. T. *Inorg. Chem.* **2005**, *44*, 5523. (b) Merlau, M. L.; Grande, W. J.; Nguyen, S. T.; Hupp, J. T. *J. Mol. Catal. A: Chem.* **2000**, *156*, 79.

Scheme 1



In this paper, we report the notable positive effects of simple dodecanethiolate-capped gold clusters on the catalytic cycle in styrene oxidation with iodobenzene (PhIO) over Mn(TPP)-Cl (TPP = tetraphenylporphyrinato). We also highlight the unique ability of gold clusters to regenerate the active forms from the once-formed Mn(IV) species with low reactivity. Thiolate-capped gold nanoclusters have been widely utilized in various settings because of their unique optical/electronic properties, easy synthesis, and high stability.<sup>9,10</sup> Although several examples of catalysts utilizing functionalized ligand shells have been reported,<sup>11</sup> there are no examples in which the activity is correlated with molecular events at the metal surface. In the present paper, we investigated the reaction and interaction involving the gold surface in detail in order to elucidate the facile catalyst reactivation by the unfunctionalized alkanethiolate-capped gold clusters.



## Results and Discussion

**Acceleration Effect of Gold Clusters in Styrene Oxidation Catalyzed by Mn–Porphyrin.** Styrene oxidation with PhIO catalyzed by Mn(TPP)Cl (Scheme 1) was examined in the presence of dodecanethiolate-capped metal clusters. Typically, the reaction was started by the addition of Mn(TPP)Cl (0.09 mM) and styrene (450 mM) after the metal cluster (0.015 mM) and PhIO (90 mM) were treated in CH<sub>2</sub>Cl<sub>2</sub> (2 mL) at 25 °C under argon for 3 h. The formation of oxidation products (styrene oxide and phenylacetaldehyde) was monitored by GC.

- (9) (a) Brust, M.; Kiely, C. J. In *Colloids and Colloid Assemblies*; Caruso, F., Ed.; Wiley-VCH: Weinheim, 2004; Chapter 3. (b) Daniel, M.-C.; Astruc, D. *Chem. Rev.* **2004**, *104*, 293. (c) Whetten, R. L.; Shafiqullin, M. N.; Khoury, J. T.; Schaaff, T. G.; Vezmar, I.; Alvarez, M. M.; Wilkinson, A. *Acc. Chem. Res.* **1999**, *32*, 397. (d) Schmid, G.; Bäuml, M.; Geerkens, M.; Heim, I.; Osemann, C.; Sawitowski, T. *Chem. Soc. Rev.* **1999**, *28*, 179.
- (10) Selected examples: (a) Brust, M.; Fink, J.; Bethell, D.; Schiffrin, D. J.; Kiely, C. J. *Chem. Soc., Chem. Commun.* **1995**, 1655. (b) Schaaff, T. G.; Shafiqullin, M. N.; Khoury, J. T.; Vezmar, I.; Whetten, R. L. *J. Phys. Chem. B* **2001**, *105*, 8785. (c) Hicks, J. F.; Miles, D. T.; Murray, R. W. *J. Am. Chem. Soc.* **2002**, *124*, 13322. (d) Negishi, Y.; Tsukuda, T. *J. Am. Chem. Soc.* **2003**, *125*, 4046. (e) Woehrl, G. H.; Brown, L. O.; Hutchison, J. E. *J. Am. Chem. Soc.* **2005**, *127*, 2172. (f) Shichibu, Y.; Negishi, Y.; Tsukuda, T.; Teranishi, T. *J. Am. Chem. Soc.* **2005**, *127*, 13464. (g) Price, R. C.; Whetten, R. L. *J. Am. Chem. Soc.* **2005**, *127*, 13750. (h) Wolfe, R. L.; Murray, R. W. *Anal. Chem.* **2006**, *78*, 1167. (i) Sweeney, S. F.; Woehrl, G. H.; Hutchison, J. E. *J. Am. Chem. Soc.* **2006**, *128*, 3190. (j) Tsunoyama, H.; Negishi, Y.; Tsukuda, T. *J. Am. Chem. Soc.* **2006**, *128*, 6036.
- (11) (a) Li, H.; Luk, Y.-Y.; Mrksich, M. *Langmuir* **1999**, *15*, 4957. (b) Pasquato, L.; Rancan, F.; Scrimin, P.; Mancin, F.; Frigeri, G. *Chem. Commun.* **2000**, 2253. (c) Manea, F.; Houillon, F. B.; Pasquato, L.; Scrimin, P. *Angew. Chem., Int. Ed.* **2004**, *43*, 6165. (d) Pengo, P.; Polizzi, S.; Pasquato, L.; Scrimin, P. *J. Am. Chem. Soc.* **2005**, *127*, 1616.

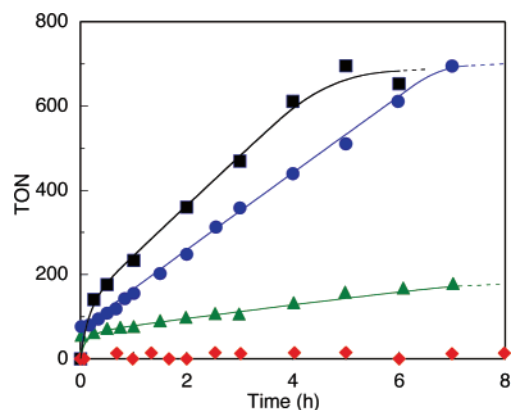


**Figure 1.** Time courses of styrene oxidation with PhIO in CH<sub>2</sub>Cl<sub>2</sub> under argon at 25 °C ([PhIO]<sub>0</sub>/[styrene]<sub>0</sub> = 90/450 mM) in the presence of Mn(TPP)Cl (0.09 mM, green ▲), Mn(TPP)Cl/1a (0.09/0.015 mM, blue ●), Mn(TPP)Cl/1b (0.09/0.001 mM, black ■), and 1a (0.015 mM, red ◆). TON = ([styrene oxide] + [phenylacetaldehyde])/[Mn(TPP)Cl]<sub>0</sub>. Cluster and PhIO were stirred in CH<sub>2</sub>Cl<sub>2</sub> for 3 h, and the reaction was then started by the addition of styrene and Mn(TPP)Cl.

**Table 1.** Catalytic Oxidation of Styrene with Various Catalyst Systems<sup>a</sup>

entry	catalyst system	[additive] <sub>0</sub> ( $\mu$ M) <sup>b</sup>	oxidant	yield (%) <sup>c,d</sup>
1	Mn(TPP)Cl	—	PhIO	17 (94/6)
2	Au:SC12 (1a)/Mn(TPP)Cl	15	PhIO	70 (75/25)
3 <sup>e</sup>	Au:SC12 (1a)/Mn(TPP)Cl	15	PhIO	44 (83/17)
4 <sup>e</sup>	Au:SC12 (1a)/Mn(TPP)Cl	15	— <sup>e</sup>	<0.1
5	Au:SC12 (1b)/Mn(TPP)Cl	0.4 <sup>f</sup>	PhIO	43 (87/13)
6	Au:SC12 (1b)/Mn(TPP)Cl	1.0 <sup>g</sup>	PhIO	69 (76/24) <sup>h</sup>
7	Au:SbN/Mn(TPP)Cl	15	PhIO	28 (85/15)
8	Pd:SC12/Mn(TPP)Cl	15	PhIO	28 (88/12)
9	Pt:SC12/Mn(TPP)Cl	1.8	PhIO	25 (94/6)
10	Ag:SC12/Mn(TPP)Cl	0.8	PhIO	27 (94/6)
11	dodecanethiol/Mn(TPP)Cl	380	PhIO	17 (93/7)
12	dodecanal/Mn(TPP)Cl	450	PhIO	23 (95/5)
13	Au:SC12 (1a)	15	PhIO	<0.1
14 <sup>e</sup>	Au:SC12 (1a)	15	— <sup>e</sup>	<0.1

<sup>a</sup> [Mn(TPP)Cl]<sub>0</sub>/[styrene]<sub>0</sub>/[PhIO]<sub>0</sub> = 0.09/450/90 mM in CH<sub>2</sub>Cl<sub>2</sub> at 25 °C under argon unless otherwise noted. <sup>b</sup> “Additive” denotes cluster, dodecanethiol, or dodecanal. <sup>c</sup> ([styrene oxide] + [phenylacetaldehyde])/[PhIO]<sub>0</sub> at 7 h. <sup>d</sup> Product ratios ([styrene oxide]/[phenylacetaldehyde]) are shown in parentheses. <sup>e</sup> Under aerobic condition. <sup>f</sup> Adjusted on the basis of the total metal atom concentration in entries 2–4. <sup>g</sup> Adjusted on the basis of the surface atom concentration in entries 2–4. <sup>h</sup> At 5 h.

In the absence of the metal clusters, the reaction took place rapidly at the very initial stage but soon after slowed down to give a TON ([oxidation products]/[Mn(TPP)Cl]<sub>0</sub>) of only 170 (17% yield based on the initial amount of PhIO) after 7 h (Figure 1, ▲; Table 1, entry 1), which is consistent with the hitherto proposed mechanism involving the transformation of initially evolved Mn(V) species into less active Mn(IV) species.<sup>6,7</sup> In contrast, when the reaction was conducted in the presence of catalytic amount (0.17 molar equiv to Mn(TPP)Cl) of dodecanethiolate-capped Au cluster with an average core diameter ( $d_{av}$ ) of 1.4 nm (Au:SC12, 1a), the TON was appreciably improved to reach ~700 (70%)<sup>12</sup> after 7 h (Figure 1, ●; Table 1, entry 2), which is approximately 4 times larger than that with Mn(TPP)Cl alone. To exclude the contribution of the fast oxidation reaction in the initial stage, the rate enhancement effect was evaluated from the TON increments between 1 and 6 h. In

- (12) The saturation of the reaction at a TON of ~700 appeared to be a result of the consumption of PhIO by the side reactions with solvent and porphyrin catalysts: (a) Smegal, J. A.; Hill, C. L. *J. Am. Chem. Soc.* **1983**, *105*, 3515. (b) Hiller, A.; Patt, J. T.; Steinbach, J. *Magn. Reson. Chem.* **2006**, *44*, 955.

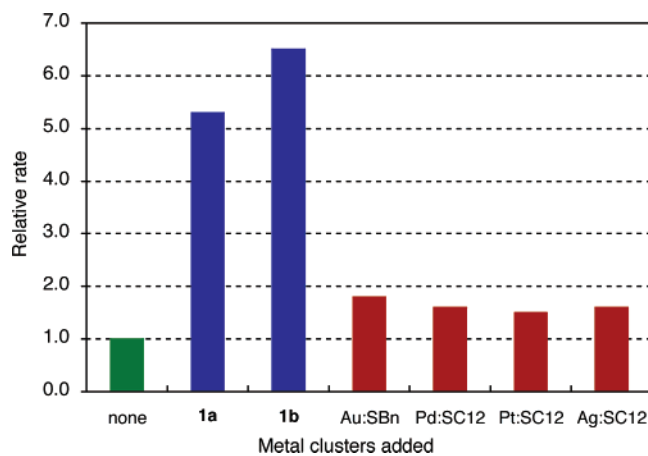


**Figure 2.** Relative rates of styrene oxidation catalyzed by Mn(TPP)Cl in the absence and in the presence of metal clusters under the reaction conditions in Figure 1 and Table 1. Rates were calculated from the time courses between 1 and 7 h, except for the reaction with **1b**, for which the data between 1 and 5 h were used.

the presence of **1a**, the reaction proceeded 5.3 times faster than the background reaction (Figure 2). A similar TON enhancement was observed when an analogous cluster with a larger average core size ( $d_{av} \approx 4.0$  nm, **1b**) was utilized at a similar gold atom concentration (Table 1, entry 5). The reaction was apparently slower than the reaction with **1a**, but it seems reasonable taking into account of their surface areas. Actually, when the concentration of **1b** was adjusted in terms of the surface area, the reaction took place similarly to **1a** (Figure 1, ■; Table 1, entry 6).

The binary catalyst system **1a**/Mn(TPP)Cl was reusable for the same reaction without loss of the original high activity. For example, when the reaction was first conducted under the condition in Figure 1 for 8 h and then styrene and PhIO were newly added to the reaction mixture, the reaction took place similarly to the first run (Figure S1, Supporting Information). On the other hand, the gold cluster **1a** alone was catalytically inert in the olefin oxidation with PhIO (Figure 1, ◆; Table 1, entry 13). Furthermore, no direct oxidation with O<sub>2</sub> (aerobic oxidation) occurred with either **1a** or **1a**/Mn(TPP)Cl (entries 4 and 14). Therefore, the gold clusters serve as promoters to accelerate the Mn–porphyrin-catalyzed oxidation by PhIO.

The remarkable acceleration effect, thus observed, was found to be specific to gold clusters. For example, the reactions in the presence of palladium (Pd:SC12), silver (Ag:SC12), and platinum (Pt:SC12) clusters took place a little faster than the background reaction, but their acceleration effects were much less significant than that of Au:SC12 (Figure 2 and Figure S2, Supporting Information). The rate enhancements over the background reaction between 1 and 8 h were at largest 1.5–1.6, which were much smaller than those with the gold clusters **1a** or **1b** (Figure 2). In connection with this, PhIO is inherently sparingly soluble in CH<sub>2</sub>Cl<sub>2</sub>, so the oxidant solubilization upon interaction with the clusters (e.g., with the alkyl chain layer via the van der Waals force) is a possible driving force of the observed acceleration. To address this point, we estimated the solubility of PhIO in CH<sub>2</sub>Cl<sub>2</sub> (2 mL) solutions of Au:SC12 and Pd:SC12 (0.045 mM). The amounts of PhIO dissolved in the cluster solutions (2.8 and 3.4 mg with Au:SC12 and Pd:SC12, respectively) were certainly larger than that in CH<sub>2</sub>Cl<sub>2</sub> alone (<1 mg), but there was no substantial difference between them.

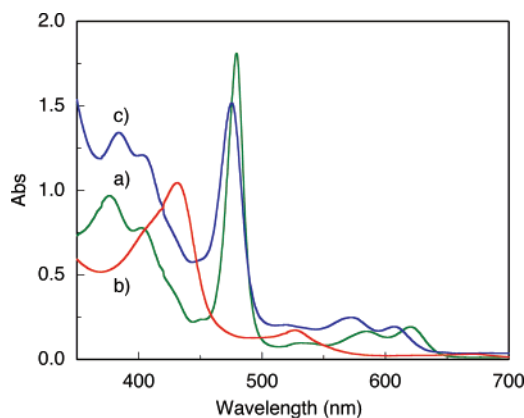


**Figure 3.** Absorption spectra in CH<sub>2</sub>Cl<sub>2</sub> at 25 °C of (a) Mn(TPP)Cl and the filtered reaction mixtures of (b) Mn(TPP)Cl and (c) **1a**/Mn(TPP)Cl after 8 h of reaction under the conditions given in Figure 1. The increase in absorbance at the short-wavelength region in spectrum c is due to the overlapping absorption of **1a**.

Therefore, the enhancement in TON is due to the specific properties of the gold clusters rather than the oxidant solubilization effect.

**Absorption Spectral Studies.** To obtain further insights into the role of the gold clusters in the observed acceleration, we measured the absorption spectrum of the catalytic system during or after the reaction. When Mn(TPP)Cl was used as a catalyst, the original bands characteristic of Mn(III)–porphyrin (478, 583, and 619 nm, Figure 3a) completely disappeared from the spectrum of the mixture after 7 h of reaction, whereas new bands due to less active Mn(IV) species were observed at 430, 525, and 666 nm (Figure 3b).<sup>7</sup> In contrast, in the presence of **1a** under otherwise identical conditions, no sign of the formation of Mn(IV) species was detected, and the spectral profile (Figure 3c) was very similar to that of the starting Mn(III) catalyst (Figure 3a), indicating the survival of the original catalytic cycle. It should also be noted that **1** can reactivate the once-formed Mn(IV) complex to convert it into active forms. For example, when the reaction was first conducted with Mn(TPP)Cl alone for 3.5 h and then **1a** was added to the reaction mixture, a remarkable rise of TON was observed after the cluster addition (Figure 4a, ●). Accordingly, the absorption bands due to the Mn(IV) species, as observed before the addition of **1a** (Figure 4b, (i)), completely disappeared, and the Mn(III) species became predominant 2.5 h after the cluster addition (Figure 4b, (ii)).

On the other hand, in the catalytic reactions coupled with the less efficient clusters Pd:SC12, Ag:SC12, and Pt:SC12, Mn(IV)–porphyrin was observed as a sole porphyrin species throughout the catalytic course. Therefore, the unique feature of the gold cluster that allows high catalytic turnovers arises from its capability to regenerate the active catalytic path involving Mn(III) and Mn(V) by transforming the less reactive Mn(IV) species into the active form.

**Reaction of Au:SC12 with PhIO.** The unique capability of the gold clusters observed is considered to be a result of molecular events at their surface. However, the metal surface of the original gold clusters **1** is densely covered by dodecanethiolate ligands, so direct interaction with the hindered porphyrin catalyst seems to be difficult. We found, by means of <sup>1</sup>H and <sup>13</sup>C NMR and GC, that the surface dodecyl groups of **1** are oxidized into aldehyde (dodecanal) by the reaction with PhIO and are eliminated from the cluster surface. The <sup>1</sup>H NMR



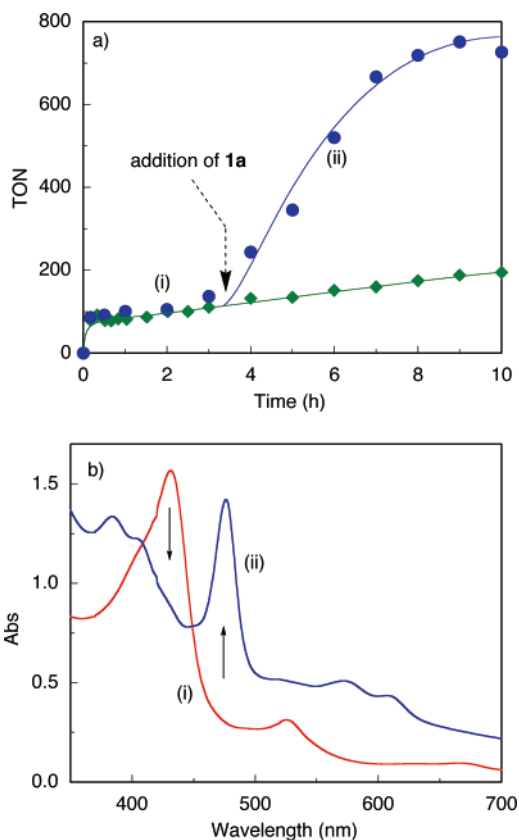


**Figure 4.** Changes of (a) the time course of the reaction (blue ●) and (b) the absorption spectrum of the reaction mixture upon the addition of **1a** (0.045 mM) after the reaction was conducted with Mn(TPP)Cl alone (0.09 mM) for 3.5 h. The result with Mn(TPP)Cl alone is also provided for comparison (a, green ◆), and traces (i) and (ii) in panel b represent the spectra at stages (i) and (ii) in panel a, respectively.

spectrum of **1a** in  $\text{CD}_2\text{Cl}_2$  upon treatment with 1000 molar equiv of PhIO showed new sharp signals due to dodecanal ( $\delta$  9.55 and 2.34 for CHO and  $\text{CH}_2\text{CHO}$ , respectively) in addition to the original broad signals of **1a** (Figure 5a). Several researchers have reported that the alkanethiolates attached to gold clusters are oxidized to disulfide or sulfonate under appropriate oxidation conditions.<sup>13</sup> In this respect, the formation of aldehyde as a result of oxidation at the  $\alpha$ -methylene of thiolate is unique, although the fate of the residual sulfur is unclear at the present stage.

The elimination of the dodecyl groups would generate an unprotected metal surface, thereby possibly causing the cluster aggregation. However, as shown in Figure 5b, the formation of dodecanal reached saturation after 3 h at  $\sim 40\%$ , where no sign of severe aggregation was observed due to the presence of the remaining dodecanethiolate ligands. Accordingly, in the absorption spectrum, the original intensity and spectral feature of the gold cluster were nearly maintained (Figure 6). The partial oxidation of dodecyl groups suggests that the thiolate reactivity varies with the attached gold sites on the cluster surface (edge, vertex, etc.).<sup>14</sup>

The reaction of **1** with PhIO appears to be a critical step associated with the acceleration/reactivation effects mediated

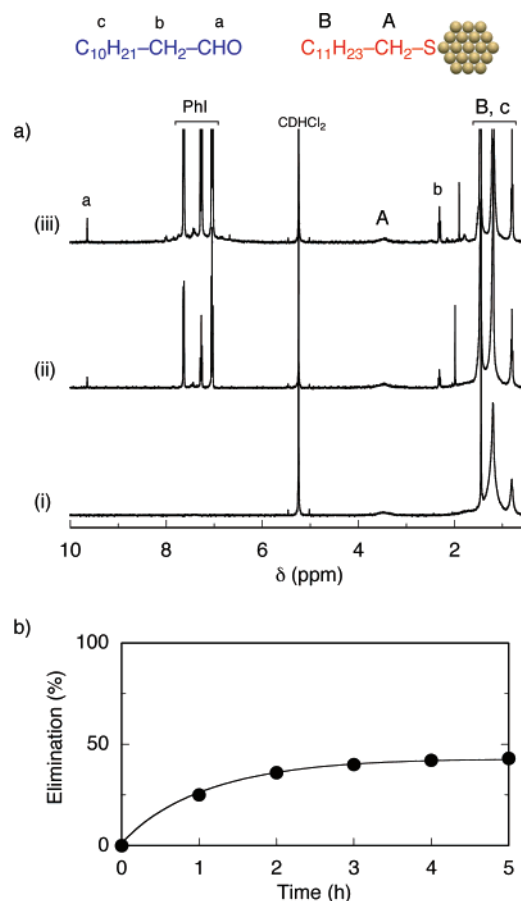


**Figure 5.** (a)  $^1\text{H}$  NMR spectra of **1a** (0.067 mM) before any reaction (i), after the reaction with 1000 equiv of PhIO for 1 h (ii), and after the same reaction for 5 h (iii) in  $\text{CD}_2\text{Cl}_2$  at 25 °C. (b) Time course of the elimination of the dodecyl group from **1a**, as estimated from the dodecanal formation in the  $^1\text{H}$  NMR spectra.

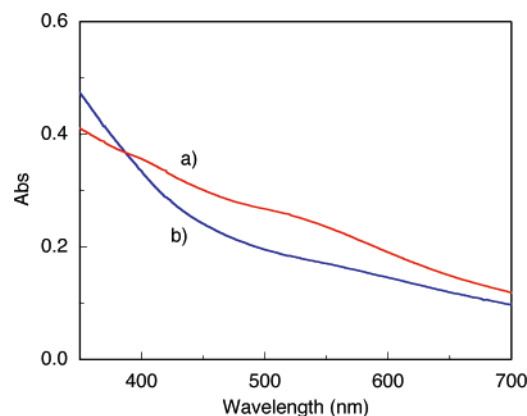


**Figure 6.** Absorption spectra of **1a** (2.6 mM in  $\text{CH}_2\text{Cl}_2$ ) before (a) and after (b) the reaction with PhIO at 25 °C.

by gold cluster **1**. In connection with this, the standard oxidation protocol we used in this study includes the pretreatment of the metal cluster with PhIO before the oxidation reaction. On the other hand, when the four components (styrene, PhIO, **1a**, Mn(TPP)Cl) were mixed “all at once”, the time course curve (Figure 7) was different from that in Figure 1 (●), giving a distorted shape with a transient plateau at about 1 h followed by a sigmoidal TON increase. This result again supports the above idea that the reaction of **1** with PhIO furnishes an important intermediate in the facile catalyst reactivation.

- (13) (a) Dasog, M.; Scott, R. W. *J. Langmuir* **2007**, *23*, 3381. (b) Schoenfish, M. H.; Pemberton, J. E. *J. Am. Chem. Soc.* **1998**, *120*, 4502. (c) Templeton, A. C.; Hostetler, M. J.; Kraft, C. T.; Murray, R. W. *J. Am. Chem. Soc.* **1998**, *120*, 1906.  
 (14) Hostetler, M. J.; Templeton, A. C.; Murray, R. W. *Langmuir* **1999**, *15*, 3782.

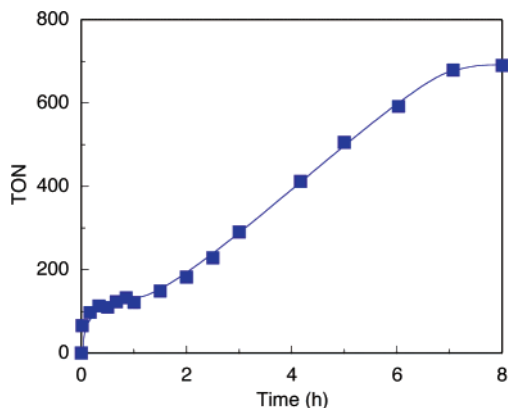


**Figure 7.** Time courses of styrene oxidation catalyzed by **1a**/Mn(TPP)Cl in CH<sub>2</sub>Cl<sub>2</sub> under argon at 25 °C ([Mn(TPP)Cl]<sub>0</sub>/[**1a**]<sub>0</sub>/[PhIO]<sub>0</sub>/[styrene]<sub>0</sub> = 0.09/0.015/90/450 mM). The four components were mixed all at once to start the reaction.

**Catalyst Reactivation on the Gold Surface: A Possible Mechanism.** As described in the above section, the reaction of **1** with PhIO affords a partially protected cluster with exposed metal surfaces (Scheme 2, **2**) and dodecanal. Dodecanal is a possible cofactor in the catalytic oxidation, but its acceleration effect was very small (Table 1, entry 12). Dodecanethiol was also inert (entry 11). Therefore, it is likely that the naked gold surface of **2** is responsible for the Mn–catalyst reactivation process. In the aerobic oxidation catalyzed by supported or polymer-protected gold nanoclusters/nanoparticles, the catalytic cycle is considered to start from the interaction of the oxidant (O<sub>2</sub>) with the gold surface.<sup>2</sup> Likewise, in our system, PhIO seems to be activated through weak Au⋯O interaction with the gold surface (**3**). Thus, Mn(IV) species generated in the catalytic cycle may be oxidized by the activated oxidant on the cluster (**3** in Scheme 2 or a subsequently formed intermediate) to give Mn(V) species. Consequently, the original catalytic cycle is revived. According to this mechanism, both O<sub>2</sub> and PhIO can interact with the naked gold surface. Since only the latter is reactive in the oxygen-atom transfer to styrene (Table 1, entry 4), O<sub>2</sub> should inhibit the reaction by competitively interacting with the gold surface. Actually, when the reaction with **1a**/Mn(TPP)Cl was conducted under aerobic conditions, a definite drop in the rate enhancement factor was observed (Table 1, entry 3).

As we have shown, Mn–porphyrin in the reaction mixture of the **1**/Mn(TPP)Cl system exists mostly in the form of Mn(III), giving spectral patterns similar to those observed with Mn(TPP)Cl. However, careful comparison reveals the obvious blue shifts of the two Q-bands (572 and 607 nm, Figures 3c and 4b, (ii)) from those of Mn(TPP)Cl. This observation suggested that Mn–porphyrin under catalytic conditions accommodated an additional axial ligand, since such shifts have been reported when coordinating bases (e.g., imidazole) were axially coordinated to Mn(III)–porphyrins.<sup>15</sup> Therefore, the above-mentioned oxidative reactivation appears to result in the linking of the cluster to Mn–porphyrin via axial ligands (**4**). In connection with this, the electron-transfer process should occur via either “inner-sphere” and “outer-sphere” mechanisms.<sup>16</sup> Considering well-known axial coordination capability of O-ligands to Mn–porphyrins, the linking formation accompanied by the electron

transfer may be facilitated by the formation of a precursor complex between the Mn(IV) species and **3** via coordinative interaction. Thus, the “inner-sphere” mechanism seems predominant in the present case, although the possibility of the “outer-sphere” mechanism that involves the transient formation of a charge-separated ionic pair is not completely excluded.

With either of the mechanisms, the hindered porphyrin catalyst must have access to the gold core that is still passivated by multiple dodecanethiolate ligands. In this context, the reaction with a gold cluster protected by less flexible and hindered benzylthiolate ligands (Au:SBn, *d*<sub>av</sub> ≈ 1.4 nm) was examined. As shown in Table 1 (entry 7) and Figure 2, Au:SBn showed a much lower co-catalyst activity than **1a** under otherwise identical conditions, suggesting that the reaction of the porphyrin catalyst with the gold core is involved in the reactivation. In the reaction with **1** protected by linear alkanethiolates, the surface groups remaining after the reaction with PhIO are not very densely packed on the surface, so they are flexible enough to accommodate the Mn–porphyrin near the cluster core.

**Effect of Au Clusters in the Oxygen-Transfer Process.** As noted above, a major role of the gold clusters in the present binary catalyst system is the oxidative reactivation of Mn(IV)–porphyrin into the active forms (Mn(III) and Mn(V)). However, it is likely that the gold clusters are also involved in the subsequent oxygen-transfer process, which was revealed by the product distribution. The styrene oxidation with PhIO catalyzed by Mn(TPP)Cl under the present reaction condition for 7 h gave styrene oxide as the main product, along with phenylacetaldehyde, with a molar ratio of 94/6. If the reactivated Mn catalyst is completely liberated from the gold surface and mediates the oxygen transfer in a free form, the product distribution should be the same as that with Mn(TPP)Cl. However, the product distribution observed with the **1a**/Mn(TPP)Cl system at 7 h was markedly different (75/25). It is known that the product distribution depends on the electronic character of the ligands surrounding the metal center.<sup>17</sup> Therefore, it is likely that the catalytic cycle predominantly turns over on Mn–porphyrin linked to the gold cluster (**4**), where the electronic effects of the gold cluster scaffold, such as the electron donation suggested in the O<sub>2</sub> activation by supported gold catalysts,<sup>2</sup> may affect the reactivity of the oxo–Mn intermediate to alter the reaction pathways.

## Conclusion

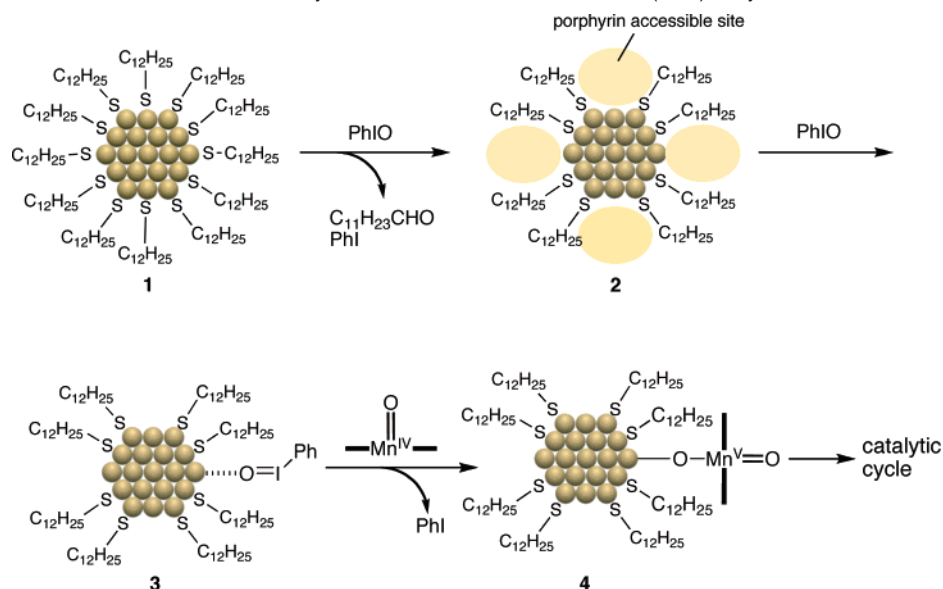
In the present paper, we have demonstrated the first example of the co-catalyst effects of gold clusters in the enhanced activity of Mn–porphyrin catalyst in the presence of simple dodecanethiolate-capped gold clusters. The uniqueness of gold clusters in the co-catalyst effect has been demonstrated in comparison with related Pd, Ag, and Pt nanoclusters. The major origin of the activity enhancement is gold-cluster-mediated regeneration of the active catalyst from catalytically ineffective Mn(IV) species. A possible mechanism that involves the “naked” (unprotected) metal surface has been presented in which the oxidant PhIO is used not only in olefin oxidation but also in the oxidative partial elimination of surface groups and subsequent Mn catalyst reactivation.

The present study not only provides an example of the additive-induced improvement of metalloporphyrin catalysis but

(15) Yuan, L. C.; Bruce, T. C. *J. Am. Chem. Soc.* **1986**, *108*, 1643.

(16) (a) Taube, H.; Gould, E. S. *Acc. Chem. Res.* **1969**, *2*, 321. (b) Kochi, J. K. *Acc. Chem. Res.* **1992**, *25*, 39.

(17) Rosenthal, J.; Pistorio, B. J.; Chang, L. L.; Nocera, D. G. *J. Org. Chem.* **2005**, *70*, 1885.

**Scheme 2.** Schematic Illustration of a Possible Catalytic Mechanism in the Au:SC12/Mn(TPP)Cl System

also demonstrates the potential utility of gold clusters for various catalytic reactions. Thiolate-capped gold clusters (monolayer-protected clusters, MPCs) have been widely utilized for biomedical and optoelectronic applications, but there have been no examples of catalysis in which the unique reactivity of the gold core is utilized. In this respect, the partially thiolate-protected cluster presented in this study has an interesting potential capability since it possesses substrate-accessible gold surfaces but is still protected from aggregation by the residual ligands. Furthermore, the residual ligands are expected to provide binding pockets near the active site. Rational design of the surface-protecting groups as well as careful choice of the agent and condition for the ligand elimination should lead to novel catalysts that show unique activity and selectivity.

## Experimental Section

**General.** Gas chromatographic (GC) analyses were performed on a Shimadzu type GC-14B instrument equipped with a flame ionization detector and a RESTEC Stabilwax PEG or Rtx-1 dimethylpolysiloxane capillary column (30.0 m  $\times$  0.25 mm  $\times$  0.25 mm). Electronic absorption spectra were measured on a JASCO type V-550 UV/vis spectrophotometer by using a quartz cell with a 1-cm path length. Laser desorption/ionization (LDI) mass spectra were obtained on a Shimadzu AXIMA-CFR linear time-of-flight mass spectrometer, where neat films of samples were prepared on a metal plate by a literature method.<sup>18</sup>  $^1\text{H}$ ,  $^{13}\text{C}$ , and  $^1\text{H}$ - $^1\text{H}$  COSY NMR spectra were measured in  $\text{CDCl}_3$  or  $\text{CD}_2\text{Cl}_2$  on a JEOL type ECX400 spectrometer, and the chemical shifts were determined with respect to internal solvent signals. Small-angle X-ray scattering (SAXS) analyses to estimate the size distribution of the clusters<sup>19</sup> were performed on a Rigaku NANO-viewer IP system for toluene solution by using a quartz capillary tube. Transmission electron micrograph (TEM) analyses were performed by Foundation for the Promotion of Material Science and Technology of Japan (MST). Samples were prepared by drop-casting a drop of toluene solution onto carbon-coated Cu grids and allowing the solvent to evaporate.

**Materials.** All solvents, including dry  $\text{CH}_2\text{Cl}_2$ , were from Kanto Chemical and were used without further purification. Hydrogen tetrachloroaurate ( $\text{HAuCl}_4 \cdot n\text{H}_2\text{O}$ ) was purchased from Furuya Metal.

Tetraoctylammonium bromide (TOAB), iodosylbenzene (PhIO), styrene, benzylthiol, and dodecanal were purchased from Tokyo Chemical Industry. Dodecanethiol and sodium borohydride ( $\text{NaBH}_4$ ) were purchased from Wako Pure Chemical Industry. The chloromanganese(III) complex of tetraphenylporphyrin [ $\text{Mn}(\text{TPP})\text{Cl}$ ] was synthesized according to a literature procedure.<sup>20</sup>  $\text{Au}_{55}(\text{PPh}_3)_{12}\text{Cl}_6$  was prepared by diborane reduction of  $\text{Au}(\text{PPh}_3)\text{Cl}$  according to a Schmidt's protocol.<sup>21</sup>

**Au:SC12** ( $d_{\text{av}} \approx 1.4$  nm) (**1a**). To a dry  $\text{CH}_2\text{Cl}_2$  solution of  $\text{Au}_{55}(\text{PPh}_3)_{12}\text{Cl}_6$  (507 mg, 0.036 mmol) was added dodecanethiol (1.0 mL, 43 mmol), and the mixture was stirred at 25  $^\circ\text{C}$  under Ar.<sup>22</sup> After 18 h, the reaction mixture was passed through a glass frit to remove black insoluble materials, and the filtrate was evaporated. The residue was suspended in acetonitrile (250 mL), and the black solids were collected by centrifugation at 3000 rpm for 15 min to give **1a** (358 mg). IR spectroscopy showed the complete disappearance of the absorption bands due to the phenyl groups of  $\text{Au}_{55}(\text{PPh}_3)_{12}\text{Cl}_6$ . TEM and SAXS analyses gave a mean diameter of 1.4 nm. LDI-MS spectrometry showed well-resolved peaks due to  $[\text{Au}_n\text{S}_m]^+$  between 8000 and 12000.<sup>10j,18</sup> Murray and co-workers have reported that a similar reaction with hexanethiol gives  $\text{Au}_{75}$  as a major product based on the LDI-MS spectrum,<sup>22c</sup> but our product is not similar since the LDI-MS signals at  $\sim 15$  000 expected for the clusters containing metal numbers of  $\sim 75$  were very small (Figure S3, Supporting Information). From elemental analysis (found: C, 21.11; H, 3.54; S, 4.34; no nitrogen was found), the averaged formula, based on the assumption that the original  $\text{Au}_{55}$  core was retained, was estimated to be  $\text{Au}_{55}(\text{SC}_{12}\text{H}_{25})_{22}$  (calcd for  $\text{Au}_{55}\text{S}_{22}\text{C}_{264}\text{H}_{550}$ : C, 20.77; H, 3.63; S, 4.62). Thermogravimetric analysis showed a mass loss of 29.4%, which agrees well with the expected organic weight fraction of 29.0% for the above formulation. LDI-MS, TEM, and SAXS profiles are provided in the Supporting Information.

**Au:SC12** ( $d_{\text{av}} \approx 4.0$  nm) (**1b**). **1b** was prepared via a modification of the Brust-Schiffrin method ( $\text{NaBH}_4$  reduction of  $\text{HAuCl}_4/\text{dodecanethiol}$  under phase-transfer conditions) reported in the literature.<sup>19</sup> SAXS or TEM analysis showed an average diameter of 4.0 nm, which was similar to those reported in the literature.

(20) Konishi, K.; Oda, K.; Nishida, K.; Aida, T.; Inoue, S. *J. Am. Chem. Soc.* **1992**, *114*, 1313.

(21) Schmid, G.; Pfeil, R.; Boese, R.; Bandermann, F.; Meyer, S.; Calis, G. H. M.; van der Velden, J. W. A. *Chem. Ber.* **1981**, *114*, 3634.

(22) (a) Brown, L. O.; Hutchison, J. E. *J. Am. Chem. Soc.* **1997**, *119*, 12384. (b) Inomata, T.; Konishi, K. *Chem. Commun.* **2003**, 1282. (c) Balasubramanian, R.; Guo, R.; Mills, A. J.; Murray, R. W. *J. Am. Chem. Soc.* **2005**, *127*, 8126.

(18) Schaaff, T. G. *Anal. Chem.* **2004**, *76*, 6187.

(19) Ito, Y.; Sasaki, A.; Sugawara, T.; Harada, G.; Nagao, O. *Jpn. J. Appl. Phys.* **2004**, *43*, 7742.

**Pd:SC12, Ag:SC12, and Pt:SC12.** Pd and Pt clusters were synthesized by  $\text{LiBEt}_3\text{H}$  reduction of  $\text{PdCl}_2(\text{CH}_3\text{CN})_2$  and  $\text{H}_2\text{PdCl}_6$ , respectively, according to the literature.<sup>23,24</sup> The Ag cluster was synthesized by  $\text{NaBH}_4$  reduction of  $\text{AgNO}_3$  in toluene according to the literature.<sup>25</sup> SAXS or TEM analysis showed average diameters of 1.4, 2.1, and 3.4 nm for the Pd, Pt, and Ag clusters, respectively, which were similar to those reported in the literature.

**Au:SBn.** Au:SBn was prepared from  $\text{Au}_{55}(\text{PPh}_3)_{12}\text{Cl}_6$  and benzylthiol in a manner similar to that described for the preparation of **1a**. The average diameter was estimated to be 1.4 nm by TEM and SAXS analyses.

In the present study, the molecular weights of the small clusters (**1a**, Au:SBn, and Pd:SC12) were estimated on the basis of the assumption that they have an  $\text{M}_{55}$  core, whereas those of the large clusters (**1b**, Pt:SC12, Ag:SC12) were estimated on the basis of the mean diameters and the bulk density.<sup>26</sup>

**Oxidation Reactions.** Typically, solid PhIO (39.6 mg, 180  $\mu\text{mol}$ ) was added to a 20 mL Schlenk tube containing a dry  $\text{CH}_2\text{Cl}_2$  solution of **1a** (0.03  $\mu\text{mol}$  in 1.8 mL) and naphthalene (~20 mg, internal standard), and the mixture was stirred at 25 °C under argon. After 3 h, a  $\text{CH}_2\text{Cl}_2$  solution of  $\text{Mn}(\text{TPP})\text{Cl}$  (0.2 mL/0.18  $\mu\text{mol}$ ) and styrene (105  $\mu\text{L}$ , 900  $\mu\text{mol}$ ) were successively added. Aliquots of the reaction

mixture were taken at appropriate intervals and subjected to GC analysis to determine the yields of the oxidation products and were subjected to absorption spectroscopy after centrifugation followed by dilution with  $\text{CH}_2\text{Cl}_2$ . After an 8 h reaction, the mixture was passed through a short silica gel column, and the  $^1\text{H}$  NMR spectrum was measured to estimate the product distribution. The above post-reaction procedures were all conducted under aerobic conditions. For the catalytic systems with other metal clusters, the surface metal numbers were adjusted to be similar to the above typical example with **1a** based on the average diameters.<sup>26</sup>

**$^1\text{H}$  NMR Monitoring of the Reaction of **1a** with PhIO.** To solid PhIO (11.5 mg, 52  $\mu\text{mol}$ ) placed in an NMR tube was added a  $\text{CD}_2\text{Cl}_2$  solution of **1a** (0.8 mg (0.05 mmol) in 0.75 mL) using a hypodermic syringe under argon, and the  $^1\text{H}$  NMR spectra were measured at 1-h intervals. The conversion of the dodecyl group into dodecanal was monitored on the basis of the integrated areas of the signals at  $\delta$  2.34 ppm due to the  $\alpha$ -methylene of dodecanal and those between 1 and 2 ppm.

**Acknowledgment.** This work is partly supported by CREST program of JST, Japan.

**Supporting Information Available:** Time courses of the reaction in the presence of Pd:SC12, Ag:SC12, Pt:SC12, dodecanal, and dodecanethiol; the result of two-stage oxidation; and characterization data of the clusters (TEM images and histograms, LDI-MS spectra, SAXS results). This material is available free of charge via the Internet at <http://pubs.acs.org>.

JA075051B

- (23) Quiros, I.; Yamada, M.; Kubo, K.; Mizutani, J.; Kurihara, M.; Nishihara, H. *Langmuir* **2002**, *18*, 1413.  
(24) Tu, W.; Takai, K.; Fukui, K.; Miyazaki, A.; Enoki, T. *J. Phys. Chem. B* **2003**, *107*, 10134.  
(25) Ellis, A. V.; D'Arcy-Gall, J.; Vijayamohan, K.; Goswami, R.; Ganesan, P. G.; Ryu, C.; Ramanath, G. *Thermochim. Acta* **2005**, *426*, 207.  
(26) Terrill, R. H.; Postlethwaite, T. A.; Chen, C.; Poon, C.; Terzis, A.; Chen, A.; Hutchison, J. E.; Clark, M. R.; Wignall, G.; Londono, J. D.; Superfine, R.; Falvo, M.; Johnson, C. S., Jr.; Samulski, E. T.; Murray, R. W. *J. Am. Chem. Soc.* **1995**, *117*, 12537.